sustainability

MDPI

Article

Wildfire Smoke, Air Quality, and Renewable Energy—Examining the Impacts of the 2020 Wildfire Season in Washington State

Augusto Zanin Bertoletti †, Theresa Phan † and Josue Campos do Prado *,†

Power System Research Group, Washington State University Vancouver, Vancouver, WA 98686, USA; a.zaninbertoletti@wsu.edu (A.Z.B.); theresa.phan@wsu.edu (T.P.)

* Correspondence: josue.camposdoprado@wsu.edu

† Current address: School of Engineering and Computer Science, Washington State University Vancouver, 14204 NE Salmon Creek Ave., Vancouver, WA 98686, USA.

Abstract: The 2020 wildfire season was devastating, setting negative records in many states and regions around the world, especially in North America. Five of the six largest fires in California's recorded history burned in 2020. In the Pacific Northwest region of the United States, Oregon and eastern Washington almost doubled their 10-year average of burnt acres recently. Depending on wind speed and direction conditions, the smoke from wildfires may significantly impact the air quality and reduce solar photovoltaic (PV) generation even in regions located hundreds of kilometers away from high-risk zones. Thus, during those periods, power system operators must ensure reliability and resilience across power generation, transmission, and distribution, while minimizing carbon emissions that can harm the air quality of the affected communities during wildfire events even more. This paper analyzes the impact of the 2020 wildfire season in the state of Washington, verifying the wind speed and solar irradiance data, and correlating these with the particulate matter 2.5 (PM 2.5) concentration and aerosol optical thickness (AOT) through a multi-variable regression model. The results show that PV production may be significantly reduced during the periods of high concentration of wildfire smoke and reduced wind speeds, thus highlighting the need for efficient and sustainable power system operations during wildfire events.

Keywords: renewable energy; resilience; wildfires; PM 2.5; AOT; air quality

check for updates

Citation: Bertoletti, A.Z.; Phan, T.; Campos do Prado, J. Wildfire Smoke, Air Quality, and Renewable Energy—Examining the Impacts of the 2020 Wildfire Season in Washington State. *Sustainability* **2022**, *14*, 9037. https://doi.org/10.3390/su14159037

Academic Editor: Diamando Vlachogiannis

Received: 1 July 2022
Accepted: 20 July 2022
Published: 23 July 2022

1. Introduction

Increasing wildfire activity in the past few years poses a threat to the reliable and resilient operation of electrical power systems around the world. The year 2020 was a vivid manifestation of several extremely severe wildfires, setting records particularly in the Arctic [1], Australia [2], Brazil [3], and the western United States (U.S.) [4].

Recent and massive wildfires in the U.S. have resulted in the loss of human life and wildlife, unhealthy air quality, destruction of property and vegetation, and billions of dollars in economic losses. In 2020, more than 50,000 wildfires were reported in the U.S. In particular, California experienced the largest wildfire season of its modern history in 2020, with more than 9000 wildfires that have burned about 4% of its 100 million acres of land [5]. A consequence of massive wildfires includes serious health effects due to short and long-term exposure to poor air quality [6], which can be analyzed by variations in particulate matter 2.5 (PM 2.5) and aerosol optical thickness (AOT) [7].

The electricity sector has been significantly affected by wildfires, which have caused large blackouts and forced many utilities to develop fire-related power shutoff programs to de-energize select transmission and distribution lines to prevent wildfires during certain weather conditions [8]. Wildfires can be naturally caused or human-induced, and there are many studies suggesting that climate change has been a key factor in increasing the risk and extent of wildfires in many regions [9–15].

However, the negative impacts of massive wildfires are not restricted to the burned areas or the areas adjacent to wildfires. Depending on the weather conditions, the smoke from wildfires can spread far beyond the burned-out site of the fire. In September of 2020, for example, the smoke from dozens of wildfires in California and Oregon stretched clear across the United States and even reached parts of Mexico, Canada, and Europe, thus diminishing air quality, and creating numerous health concerns [16]. Figure 1 illustrates the smoke dispersion layers from the U.S. National Oceanic and Atmospheric Administration (NOAA) Hazard Mapping System (HMS) on 9 September 2020.

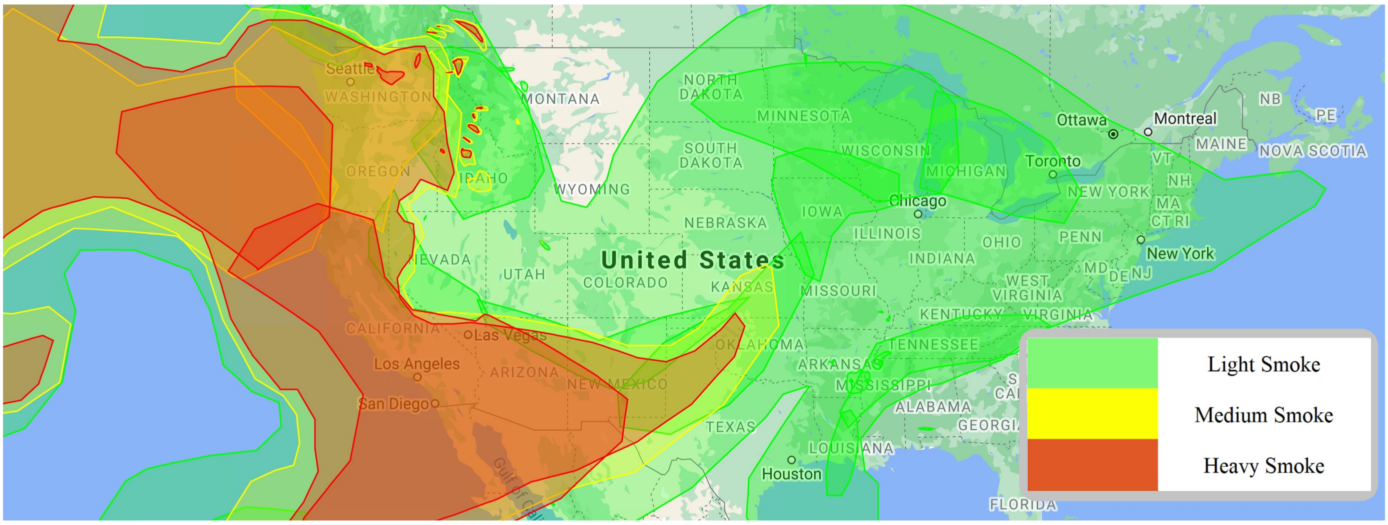

Figure 1. The span of smoke from wildfires on 9 September 2020. Smoke layers are from the NOAA HMS [17]. Map data from Google [18].

As far as 1000 km away, wildfire smoke can increase ambient air and worsen the associated risks of illness and death [19]. Moreover, the smoke from wildfires can significantly reduce solar irradiance and, thus, lead to a decrease of solar-powered electricity generation, especially in periods of lower wind speeds. This is particularly concerning for regions and countries with increasing integration of renewable energy sources. Several wildfires in California led to a 13% decrease in solar power generation in 2020 in the region operated by California Independent System Operator (CAISO) [20]. Renewables made up nearly 20 percent of utility-scale U.S. electricity generation in 2020, with the bulk coming from hydropower (7.3%) and wind power (8.4%); solar generation, the fastest-growing electricity source [21], made up 3.3% of total U.S. generation in the same year.

However, the existing research works on the impacts of wildfire smoke on renewable power generation are surprisingly limited. The work in [22] tracked the increase of aerosols in the atmosphere since the early 2000s, showing the impact of the rising AOT on solar production, specially in California, in 2020. In [23,24], the authors studied the correlations between solar PV generation and the PM 2.5 in California during recent wildfire events. In [25], a solar photovoltaic (PV) capacity model was developed to quantify the anticipated temporal reduction in solar power capacity due to wildfire smoke. In this work, the authors considered the AOT to quantify the amount of smoke present at a specific point in time and developed a simple linear regression model. To the best of the authors' knowledge, none of the existing works considered both the PM 2.5 and the AOT to estimate the reduction of solar power generation. Moreover, the existing literature did not analyze the wind speed conditions during the periods of high concentration of wildfire smoke and deteriorated air quality.

This paper analyzes the impact of the 2020 wildfire season in the state of Washington and proposes a multi-variable linear regression model to analyze the correlation between the PM 2.5 and AOT and the sun irradiance for six different locations across the state. Furthermore, the wind speed is analyzed during the same period, verifying the conditions for renewable energy generation during the periods of intense wildfire activity. The contributions of this paper are summarized as follows:

- A comprehensive analysis of the impacts of the 2020 wildfire season on renewable energy in Washington state, focusing on variables that directly impact the wind and photovoltaic power, is provided. To the best of the authors' knowledge, this is the first work that analyzed both solar radiation and wind speeds in periods of significant wildfire smoke activity.
- A multi-variable linear regression model is developed to predict sun irradiance during wildfire activity periods, considering both the PM 2.5 and the AOT.

The remainder of this paper is organized as follows: Section 2 details the 2020 wildfire season in the state of Washington; Section 3 describes the methodology used to study the impacts of wildfire smoke on renewable energy; Section 4 presents the results from the analysis; and finally, Section 5 presents the conclusions, discussing important implications for power systems affected by wildfire smoke.

2. 2020 Washington State Wildfire Season

In this work, the period between 31st August and 21st September of 2020 was analyzed. Six locations in different parts of the state of Washington were considered: Everett, Long Beach, Pullman, Puyallup, Spokane, and Wenatchee.

The pronounced warm and dry period in the early months of 2020 resulted in early season fire activity in April [26]. In July, the conditions were even worse, with no measurable precipitation and moderate and severe droughts in the center and the southwest parts of the state. In the following month, only a single wetting rain across most of the state, on 6 August, was recorded. The month of September began with a very strong thermal drought, bringing hot and dry conditions for a prolonged period of time. On Labor Day weekend, there was an alignment of critical fuels, critical weather, and abundant new ignitions [26]. In September 2020, there were 18 fires in the state of Washington that were considered large and/or significant [27]. The amount of acres burned due to those fires are presented in Figure 2.

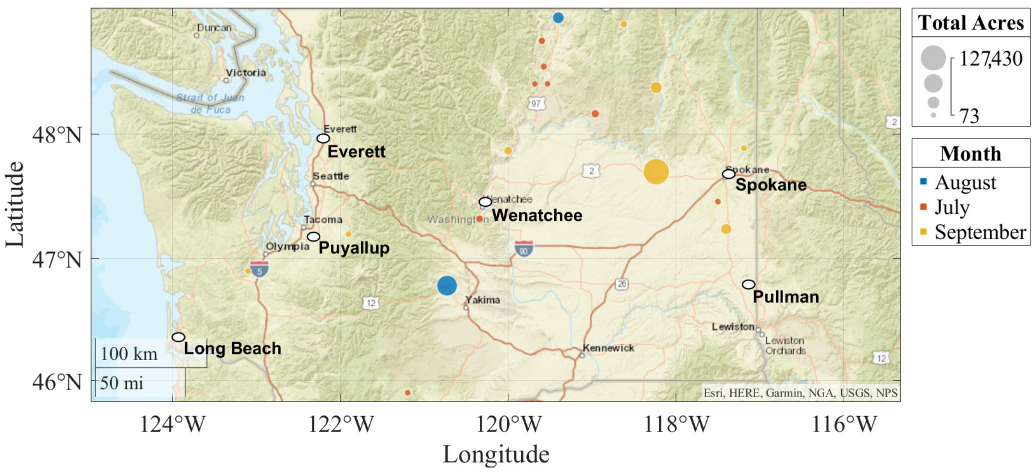

Figure 2. Geographical localization of all the analyzed cities in this work, and total acres burned due to large fires in the state of Washington, during the months of July, August, and September.

The fires presented in Figure 2 burned over 273,000 acres across federal, private, state, and tribal ownership. According to the Washington State Department of Natural Resources (DNR), over 150,000 acres were burned in September 2020. The largest fire registered for the state of Washington in the analyzed period was the Whitney fire, which burned over 125,000 acres near Davenport, WA, in Lincoln County [27].

The smoke from those major wildfires spread across the western U.S., later entering the jet stream and traveling across the Atlantic Ocean, as illustrated in Figure 1. On 9th

September, the states of Washington, Oregon, and California were completely covered by a heavy layer of smoke. The high smoke concentration of particulates in the atmosphere directly impacted the solar irradiance at lower altitudes in those locations.

3. Methodology

This section presents the approach taken to examine the technical impacts of the 2020 wildfire season on renewable energy in the state of Washington.

During the 2020 wildfire season, the air quality index (AQI) and the AOT levels were analyzed for PV generation and considered as independent variables in the multi-variable regression model presented in Section 3.1.2. For the wind generation, the distribution of the wind speeds in the same period is examined in order to study the behavior of wind speeds during the periods of high concentration of wildfire smoke and understand the associated implications for power system operation.

3.1. Photovoltaic Generation

3.1.1. PVWatts Model

PV generation is dependent on specifications of a given cell array and climate factors (e.g., sun irradiance and temperature), as presented in the PVWatts [28] model. The model computes the maximum DC power from the array given a computed cell temperature and solar irradiance. The array efficiency is assumed to decrease at a linear rate as a function of temperature rise, governed by a temperature coefficient. The reference cell temperature is 25 °C, and reference irradiance is 1000 W/m^2. The equation for DC power is presented in (1). However, the variables presented in (1) can be affected by other meteorological variables, as presented in [29].

$$P_M = \frac{I_{tr}}{I_{ref}} P_{ref}\left(1 + \gamma\left(T_{cell} - T_{ref}\right)\right) \tag{1}$$

where

- P_M : maximum power point (W);
- P_{ref}: maximum power point at reference solar radiation (W);
- I_{tr}: solar radiation received on module plane (W/m^2);
- I_{ref}: reference solar radiation;
- γ: temperature correction coefficient;
- T_{cell}: cell/module operating temperature (°C);
- T_{ref}: reference temperature.

In order to study the impact of wildfire smoke on the expected PV capacity, the sun irradiance is analyzed during the 2020 wildfire season. The *i*th value is normalized to values from 0 to 1, allowing comparison between different locations, as presented in (2).

$$I'_{tr_i} = \frac{I'_{tr_i} - I_{tr,min}}{I_{tr,max} - I_{tr,min}} \tag{2}$$

where, I'_{tr}, $I_{tr,\,max}$, and $I_{tr,\,min}$ are the normalized, maximum, and minimum sun irradiance values during the studied period.

3.1.2. Wildfire Smoke PV Regression Model

Wildfire smoke contains small, airborne particulate matter particles that are generally 2.5 μm or smaller (referred to as PM 2.5) [24]. This matter reduces the amount of sunlight that reaches solar panels, decreasing solar-powered electricity generation. The U.S. Environmental Protection Agency (EPA) updated the Air Quality Index (AQI) for PM 2.5, in 2012, using a color-based tool for different air quality levels [30]. The upper end, considered as *good* air quality, considers a concentration less than 12 μg/m^3. On the other hand, a concentration higher than 250.5 μg/m^3 indicates hazardous conditions. All AQI categories along with the corresponding range and colors are presented in Table 1.

Table 1. AQI breakpoints, revised in 2012 by the EPA. Table adapted from [30].

PM 2.5 AQI Category	PM 2.5 Levels (μg/m^3)	Color
Good	0.0–12.0	
Moderate	12.1–35.4	
Unhealthy for Sensitive Groups	35.5–55.4	
Unhealthy	55.5–150.4	
Very Unhealthy	150.5–250.4	
Hazardous	≥250.5	

Furthermore, during the periods of high wildfire smoke concentration, the AOT tends to increase, being used to quantify the distribution and density of wildfire smoke [31]. The AOT is the degree to which aerosols prevent the transmission of light by absorption or scattering of light. It has no unit, with an average values from 0.1 to 0.15 for the U.S [32].

When looking at the overall relationship between AOT and normalized PV capacity, there is a generally linear relationship [25]. Therefore, a multiple regression analysis is proposed, considering both the AOT and the PM 2.5 to estimate the reduction in PV generation when wildfire smoke is present. The sun irradiance values between 11 a.m. and 1 p.m. are extracted from the assessment period in order to consider the impact on the peak PV capacity.

After removing outliers, a simple regression model is used, as presented in (3):

$$f(x) = a_1 + a_2 x_1 + a_3 x_2 \tag{3}$$

where a_1 is the intercept, a_2 the coefficient for the AOT variable, and a_3 is the coefficient for the PM 2.5. To analyze the accuracy of the proposed model, the mean absolute error (MAE) metric and the mean squared error (MSE) are calculated.

3.1.3. ANOVA for Regression

During high-density wildfire smoke conditions, both the AOT and the PM 2.5 AQI are significantly elevated, thus impacting the sun irradiance value. To verify its significance, we use single-factor ANOVA analysis. This tool determines whether the independent variable has a significant impact on the value of a dependent variable [33].

The calculations performed for the ANOVA analysis are presented in Table 2, where

- df: degrees of freedom.
- SS: sum of Squares.
- MS: mean Squares.
- F: variation within samples.
- N: the number of samples.
- I: the number of samples means.
- F_{crit}: the value of the F-statistic at the threshold probability α of mistakenly rejecting a true null hypothesis.

Table 2. The analysis of variance table for regression, adapted from [33].

Source	*df*	*SS*	*MS*	*F*
Model	$I-1$	$\sum(\hat{y}_i - \bar{y})^2$	SS_M/df_M	MS_M/MS_E
Residual	$N-I$	$SS_T - SS_M$	SS_R/df_R	
Total	$N-1$	$\sum(\bar{y}_{ij} - \bar{y})^2$		

The null hypothesis (applies if $F < F_{crit}$) in this case reads as follows: the mean values are the same, that is, the values of the independent variables (AOT and PM 2.5 AQI) do not affect the values of the dependent variable (sun irradiance). The alternative hypothesis (applies if $F > F_{crit}$) reads as follows: the mean values of the selected variables differ, that is, the value of the independent variables affect the value of the dependent variable. The analysis is carried out for all the selected locations.

3.2. Wind Generation

The power output of a wind turbine has a direct relation with the cross-section area of the turbine's blades (A), the air density (ρ), and the cubic of the wind speed (U) [34], as shown in (4). The wind turbine rotor performance is usually characterized by its power coefficient, C_P, the ratio of the rotor power, and the wind power.

$$P = \frac{1}{2}\rho A U^3 \tag{4}$$

In this study, the wind speeds in all six selected locations are analyzed during periods with different concentrations of wildfire smoke in order to study the potential impacts on wind power generation and potential implications to power system operation during wildfires.

4. Data and Results

This section presents an analysis of the impact of the 2020 wildfire season on renewables in the state of Washington.

4.1. Data

Figures 3–8 present the solar irradiance and the wind speed values for Everett, Long Beach, Pullman, Puyallup, Spokane, and Wenatchee, respectively, during the studied period. The data was obtained from the Washington State University (WSU) AgWeatherNet (AWN) database, which contains various weather-related data from different weather stations across the state of Washington [35]. Note that, during the third week of September of 2020, the sun irradiance and wind speed levels were remarkably low, thus negatively impacting the wind and solar power production in those locations.

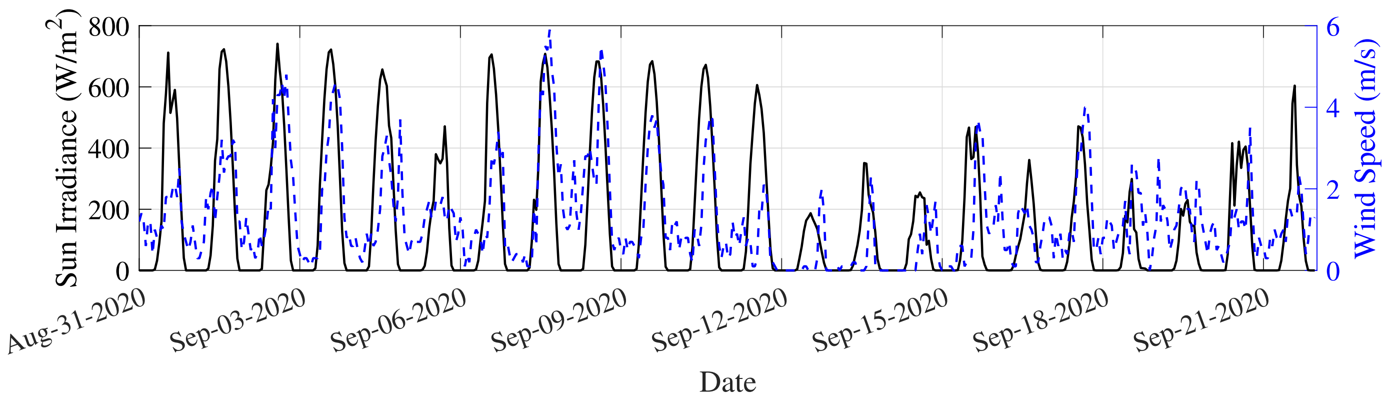

Figure 3. Solar irradiance (W/m^2) and wind speed (m/s) during the first three weeks of September of 2020, in Everett, WA.

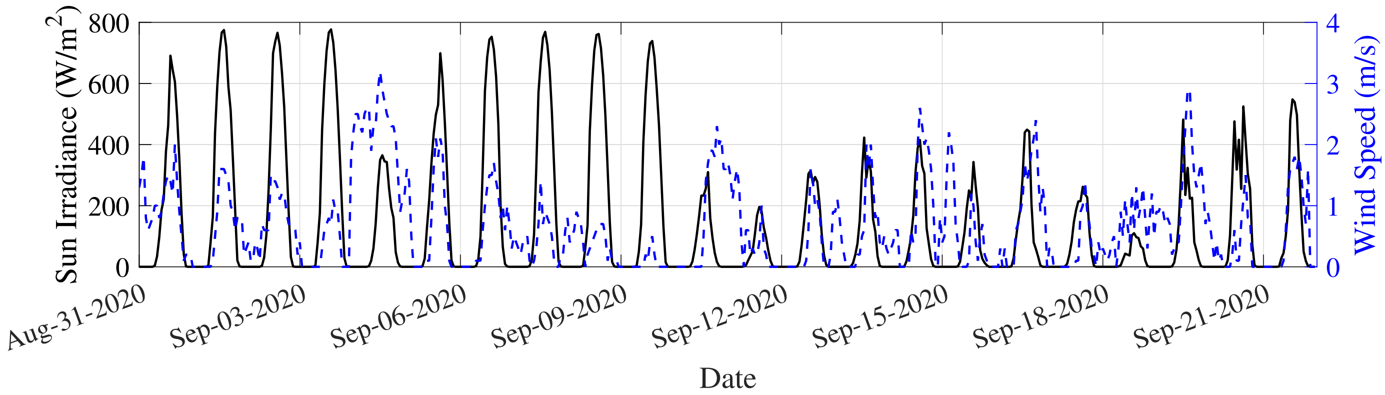

Figure 4. Solar irradiance (W/m^2) and wind speed (m/s) during the first three weeks of September of 2020, in Long Beach, WA.

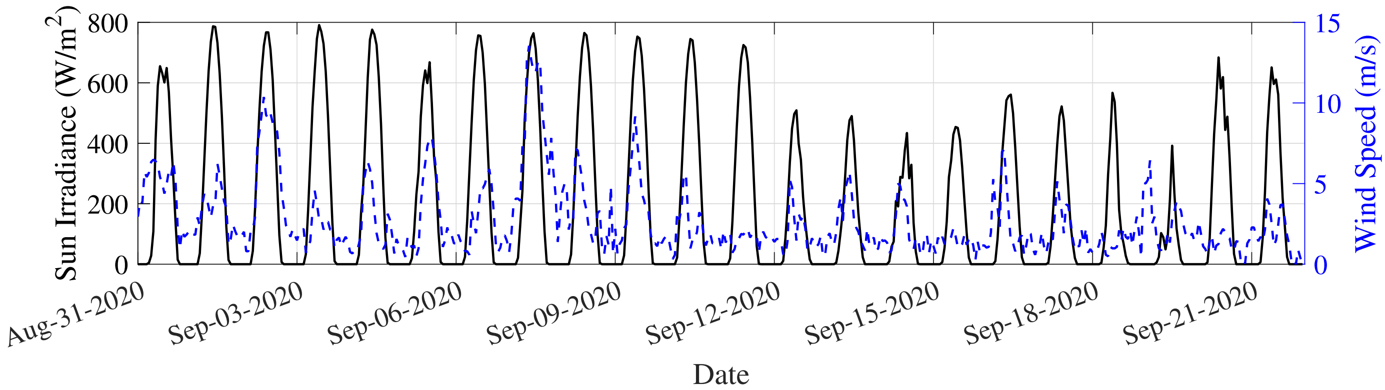

Figure 5. Solar irradiance (W/m^2) and wind speed (m/s) during the first three weeks of September of 2020, in Pullman, WA.

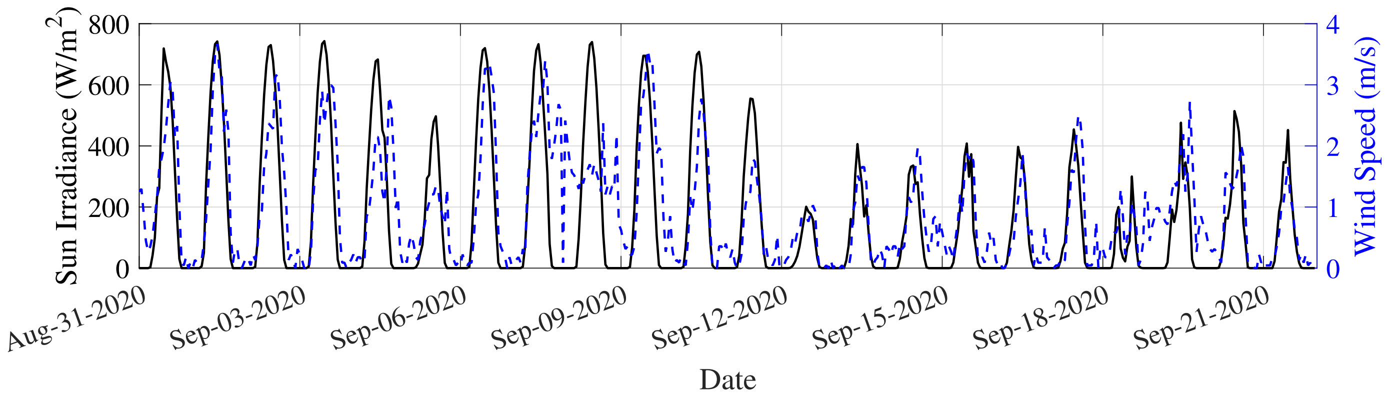

Figure 6. Solar irradiance (W/m^2) and wind speed (m/s) during the first three weeks of September of 2020, in Puyallup, WA.

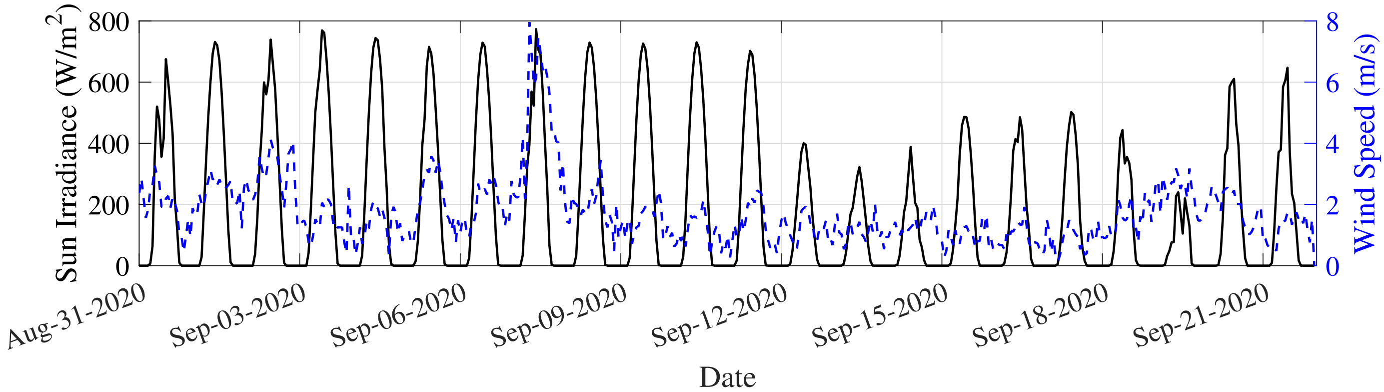

Figure 7. Solar irradiance (W/m^2) and wind speed (m/s) during the first three weeks of September of 2020, in Spokane, WA.

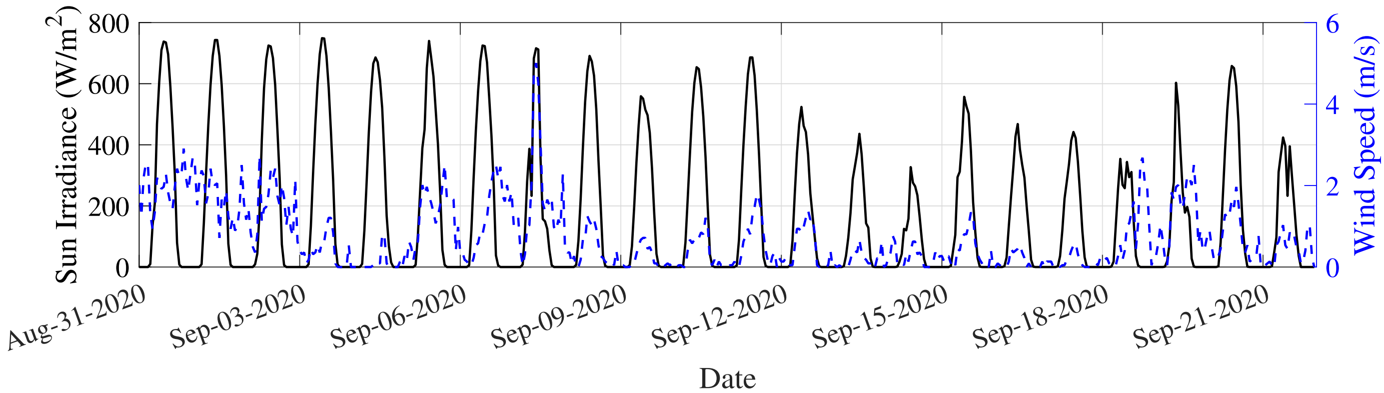

Figure 8. Solar irradiance (W/m^2) and wind speed (m/s) during the first three weeks of September of 2020, in Wenatchee, WA.

During the first three weeks of September of 2020, an abrupt increase in the AOT and PM 2.5 was observed, for the analyzed locations. Figure 9a presents the PM 2.5 hourly averaged values for the analyzed locations, during the first three weeks of September of 2020. The data was obtained from the Washington State Department of Ecology, available in [36]. The highest PM 2.5 value during the analyzed period was for the city of Spokane, reaching more than 430 µg/m^3. It turned out that the peak PM 2.5 values occurred during the lowest period of sun irradiance for all locations, in the beginning of the third week of September.

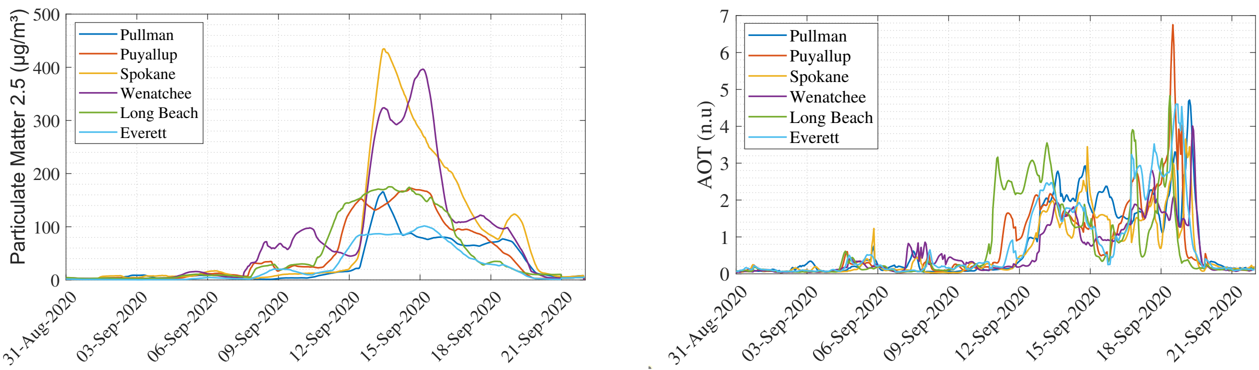

(**a**) (**b**)

Figure 9. (**a**) PM 2.5 and (**b**) AOT values for the locations analyzed, during the first three weeks of September 2020.

Figure 9b presents the AOT values, collected from the Modern-Era Retrospective analysis for Research and Applications, Version 2 (MERRA-2), available in [37]. It turned out that, after 11 September 2020, the AOT increased significantly in all analyzed locations in the state of Washington. The highest AOT levels were measured in Puyallup, which also experienced the highest sun irradiance variations, as previously shown in Figure 6.

Figure 10 shows the air quality conditions throughout the analyzed period for the six locations. The category is represented by the same colors indicated in Table 1. With the exception of Pullman and Everett, all the other locations were subject to undesirable air quality conditions during more than half of the period considered. For Spokane and Wenatchee, the air quality reached hazardous levels, staying that way for at least a day.

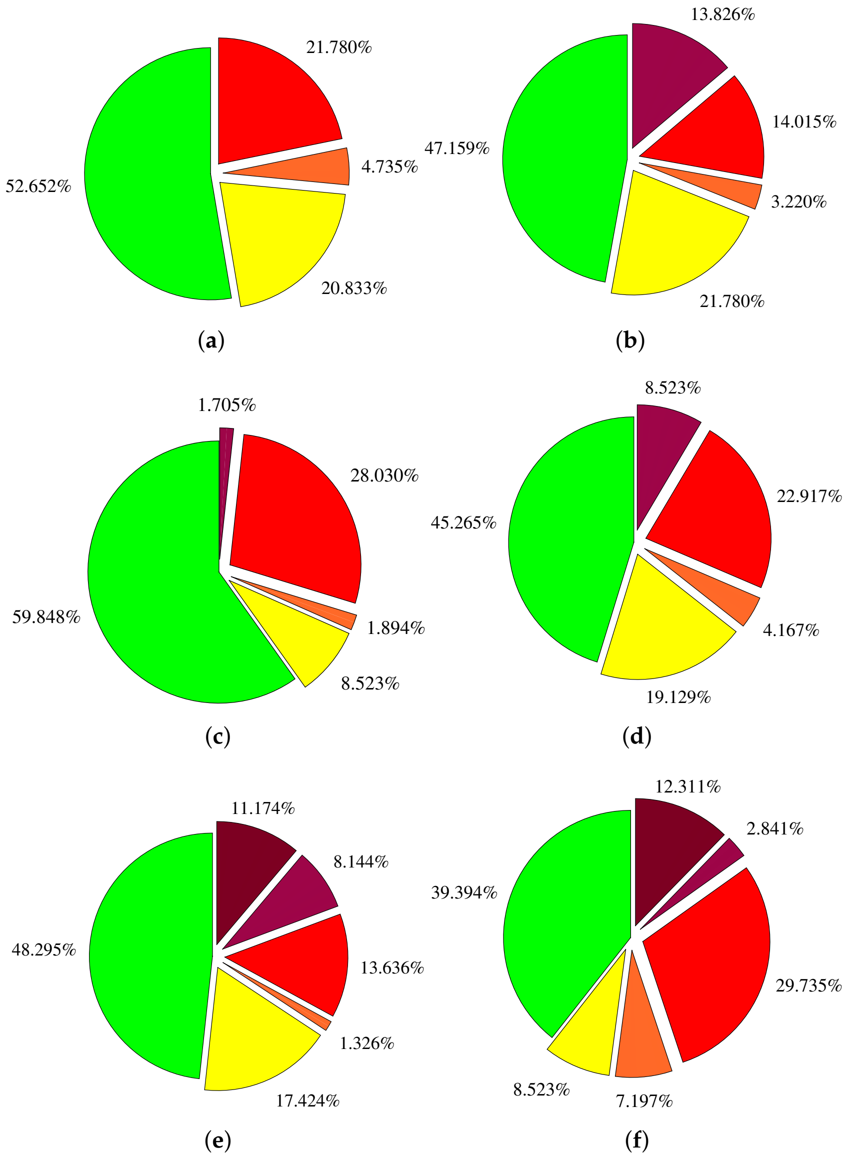

Figure 10. PM 2.5 level distribution during the first three weeks of September 2020 for the cities of (**a**) Everett, (**b**) Long Beach, (**c**) Pullman, (**d**) Puyallup, (**e**) Spokane, and (**f**) Wenatchee.

4.2. Solar Photovoltaics

Tables 3–8 show the results of the ANOVA analysis. In all cases, the values of F are higher than the F_{crit} (for a confidence of 1%), thus confirming that the variables affect the value of the sun irradiance. The highest value of F (i.e., 75.98) was obtained in Pullman. On the other hand, Everett recorded the lowest value (i.e., 18.5516).

The decrease in solar irradiance and, consequently, the reduction in PV generation were analyzed using scatter plots and their regression in a multi-variable linear model for each studied location. After removing outliers, a total of 63, 59, 59, 61, 61, and 60 points were fitted to a multiple linear regression model, for the cities for Everett, Long Beach, Pullman, Puyallup, Spokane, and Wenatchee, respectively.

Table 3. ANOVA analysis for regression for the city of Everett, WA.

	df	*SS*	*MS*	*F*	F_{crit}
Regression	2	1.7886	0.8943	18.5516	0.9513
Residual	60	2.8924	0.0482		
Total	62	4.6810			

Table 4. ANOVA analysis for regression for the city of Long Beach, WA.

	df	*SS*	*MS*	*F*	F_{crit}
Regression	2	2.0623	1.0311	21.3452	0.9513
Residual	56	2.7052	0.0483		
Total	58	4.7675			

Table 5. ANOVA analysis for regression for the city of Pullman, WA.

	df	*SS*	*MS*	*F*	F_{crit}
Regression	2	1.8183	0.9092	75.9726	0.9513
Residual	56	0.6701	0.0120		
Total	58	2.4885			

Table 6. ANOVA analysis for regression for the city of Puyallup, WA.

	df	*SS*	*MS*	*F*	F_{crit}
Regression	2	1.9639	0.9820	43.1779	0.9513
Residual	58	1.3190	0.0227		
Total	60	3.2829			

Table 7. ANOVA analysis for regression for the city of Spokane, WA.

	df	*SS*	*MS*	*F*	F_{crit}
Regression	2	1.6905	0.8453	50.6302	0.9513
Residual	58	0.9683	0.0167		
Total	60	2.6588			

Table 8. ANOVA analysis for regression for the city of Wenatchee, WA.

	df	*SS*	*MS*	*F*	F_{crit}
Regression	2	1.3400	0.6700	29.7382	0.9513
Residual	57	1.2842	0.0225		
Total	59	2.6241			

In order to validate the statistical assumptions made in the methodology, the variance inflation factor (VIF) is used as an indicator of multicollinearity between the independent variables (i.e., AOT and PM 2.5). The results indicate VIF of 1.7739, 2.3866, 4.3863, 1.8742, 2.0715, and 1.4604, for Everett, Long Beach, Pullman, Puyallup, Spokane, and Wenatchee, respectively. Given that all VIFs < 5, no considerable collinearities were identified [38].

The results are presented in Figure 11a–f, for Everett, Long Beach, Pullman, Puyallup, Spokane, and Wenatchee, respectively. The error metrics for all models are presented in Table 9. The best fit was for the city of Pullman, with an MSE and r^2 of 8.91% and 0.73, respectively. On the other hand, the fit for the city of Everett presented the highest MSE value of 18.24% and the lowest r^2 value of 0.38.

When analyzing the relation between the AOT and PM 2.5 and the normalized sun irradiance, there is a generally linear relationship, which justifies the fit. Since the analyzed period starts roughly a week and a half before high-intensity wildfire activity, many points with small values of AOT and PM 2.5 were observed.

Note that, under normal conditions (i.e., AOT levels lower than 0.1 and PM 2.5 levels lower than 12), the estimated sun irradiance was slightly greater than 0.8 for Long Beach, Puyallup, Spokane, and Wenatchee, and sightly greater than 0.7 for Everett. However, the proposed model presented a satisfactory performance for higher AOT and PM 2.5 levels, thus indicating a significant reduction in solar irradiance and PV power generation during periods of high wildfire smoke concentration.

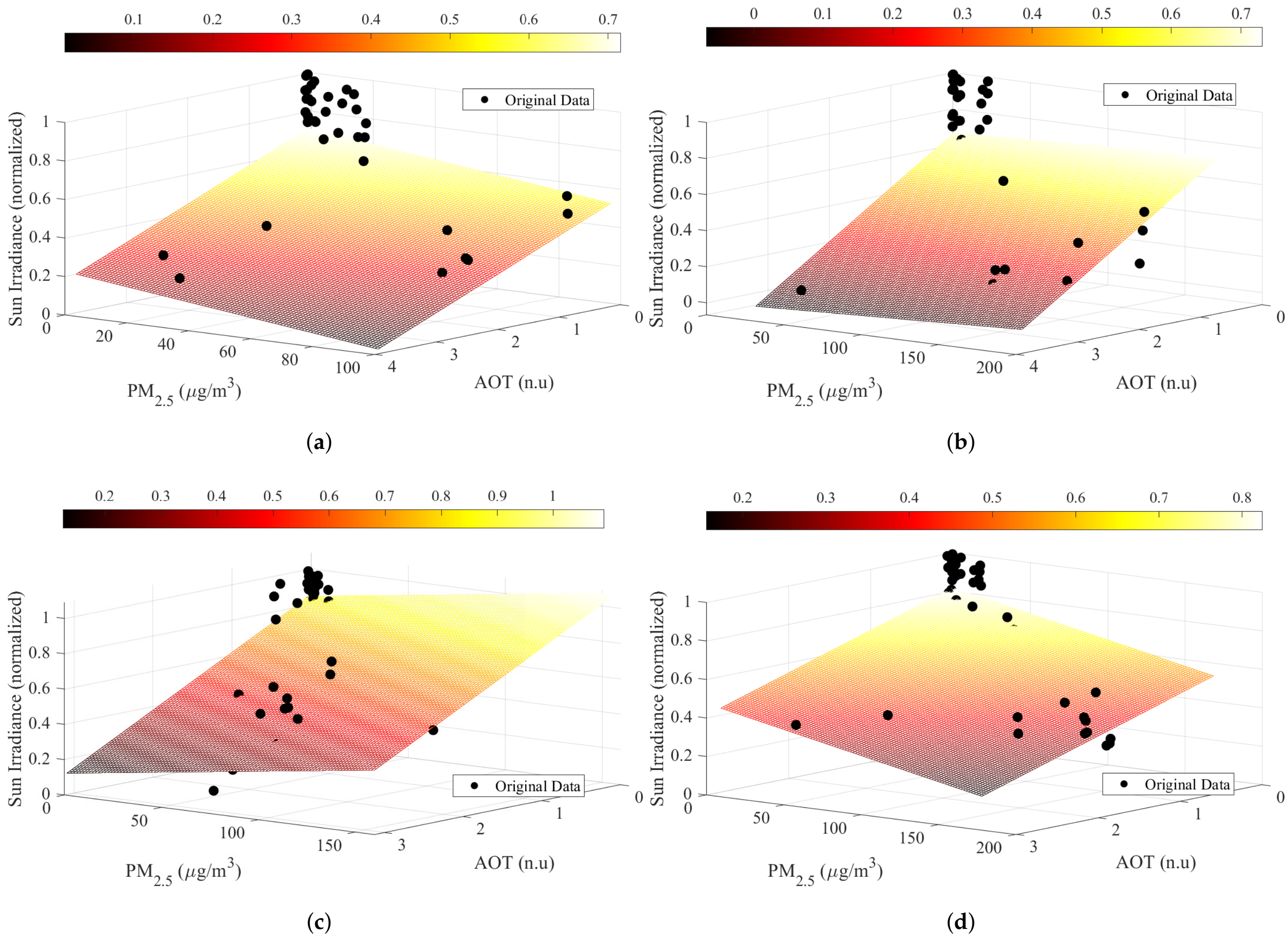

Figure 11. *Cont.*

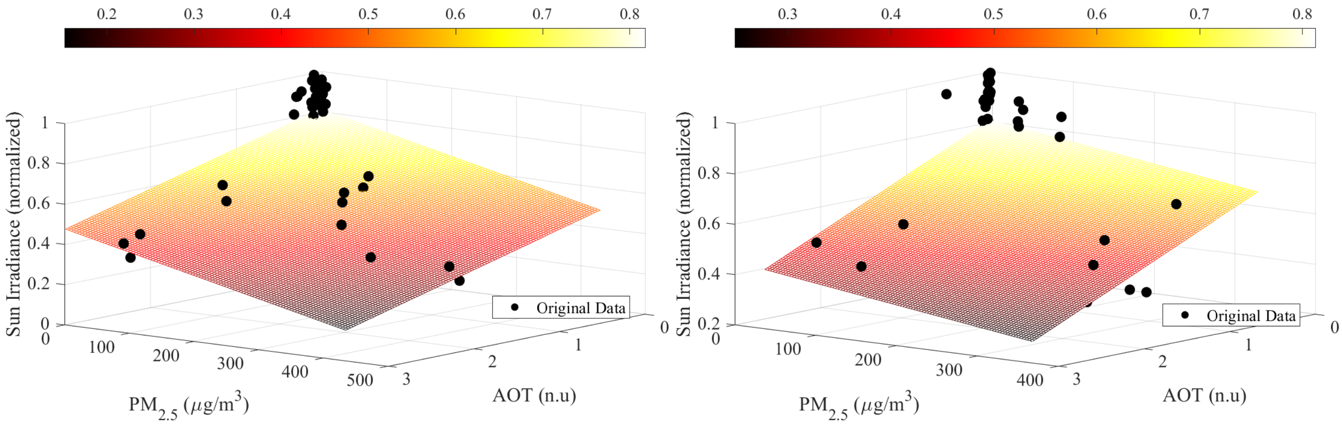

(e) **(f)**

Figure 11. Multiple linear regression analysis between the solar irradiance, the AOT, and the PM 2.5 data during the 2020 wildfire season for the cities of (**a**) Everett, (**b**) Long Beach, (**c**) Pullman, (**d**) Puyallup, (**e**) Spokane, and (**f**) Wenatchee.

Table 9. MAE and MSE values for the sun irradiance multiple regression linear model for the analyzed cities.

City	Everett	Long Beach	Pullman	Puyallup	Spokane	Wenatchee
MAE (%)	18.24	18.19	8.91	12.13	10.25	12.05
r^2	0.38	0.43	0.73	0.59	0.63	0.51

4.3. Wind Speeds

In this section, we analyze the wind speeds and the associated impacts on wind power generation during periods with different AQI levels. Figure 12a shows the wind speed average decrease when the AQI changed from *good* to worse conditions. The percentage difference for all categories in relation to normal conditions is plotted for all locations, as illustrated in Figure 12b. The location with the worst decay in average wind speed was Wenatchee. When comparing *very unhealthy* PM 2.5 AQI samples with normal conditions, the average wind speed decreased almost 93%. The city of Spokane presented average speed decay, in relation with good AQI samples, for all categories, with almost 53% for very unhealthy.

Among all analyzed locations, Everett and Pullman were the locations whose AQI values were predominantly *good* during the analyzed period. However, in Pullman, the average wind speed decreased by about 38% when comparing all the samples with a PM 2.5 AQI higher than 12 μg/m^3, and by 29.80% for the city of Everett. In Pullman, the average wind speed during *good* AQI conditions was 52% higher than the average wind speed during *unhealthy for sensitive groups* AQI conditions. The same behavior was observed for all analyzed locations. The wind speed histograms were split according to each PM 2.5 AQI category shown in Table 1. A total of 528 points were obtained for each location. Figure 13a–f present the wind sped histograms for Everett, Long Beach, Pullman, Puyallup, Spokane, and Wenatchee, respectively. The average wind speeds, in meters per second, for the analyzed period are presented in Table 10.

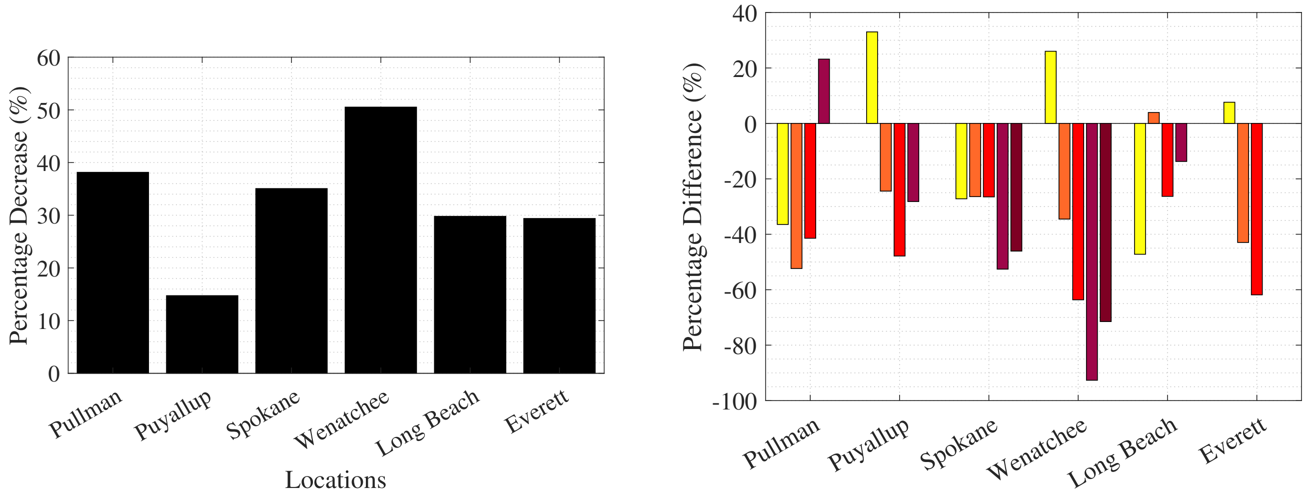

(**a**) (**b**)

Figure 12. (**a**) Wind speed average percentage decrease for the analyzed locations, comparing periods below and above the good PM 2.5 AQI breakpoint, and the (**b**) wind speed average percentage difference for the analyzed locations, comparing all PM 2.5 AQI breakpoints with normal condition.

Table 10. Wind speeds (m/s) for all the analyzed locations, during different air quality conditions.

City	Everett	Long Beach	Pullman	Puyallup	Spokane	Wenatchee
	1.465	0.792	3.189	1.003	2.100	1.056
	1.577	0.418	2.027	1.334	1.529	1.331
	0.836	0.823	1.520	0.758	1.545	0.692
	0.559	0.584	1.868	0.523	1.544	0.384
	-	0.684	3.929	0.720	0.996	0.077
	-	-	-	-	1.133	0.301

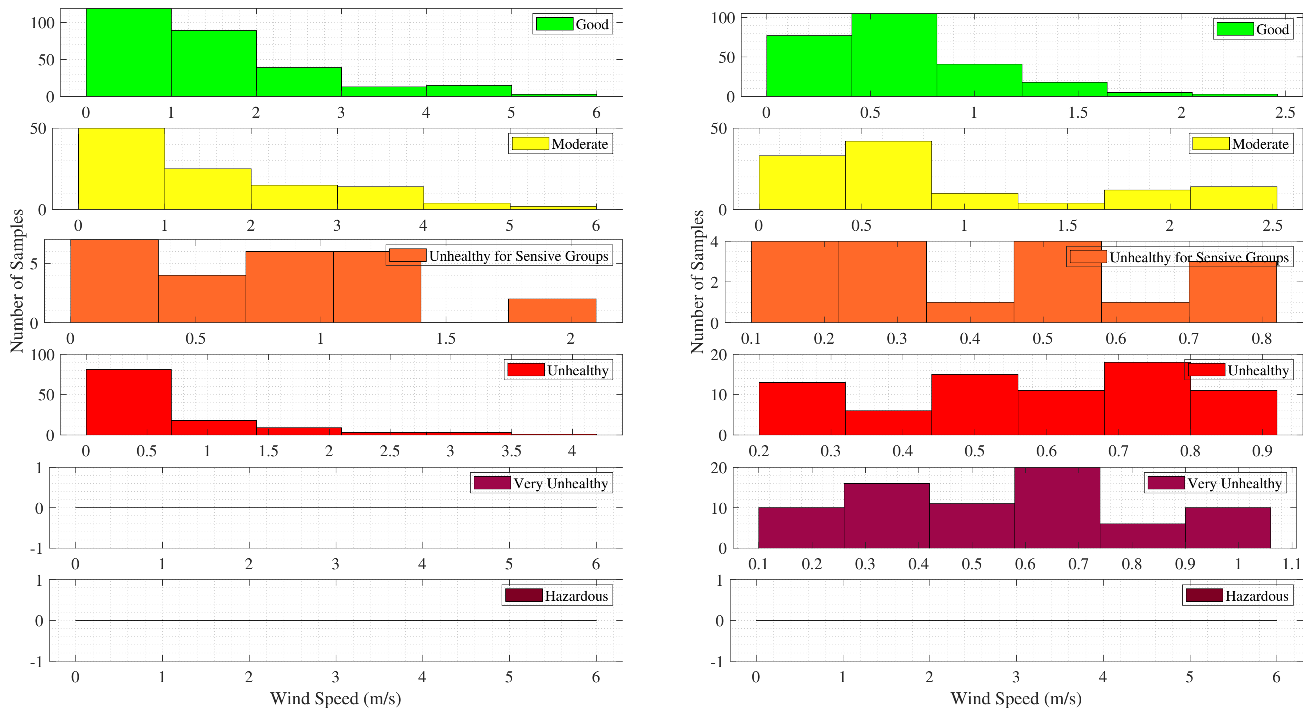

(**a**) (**b**)

Figure 13. *Cont.*

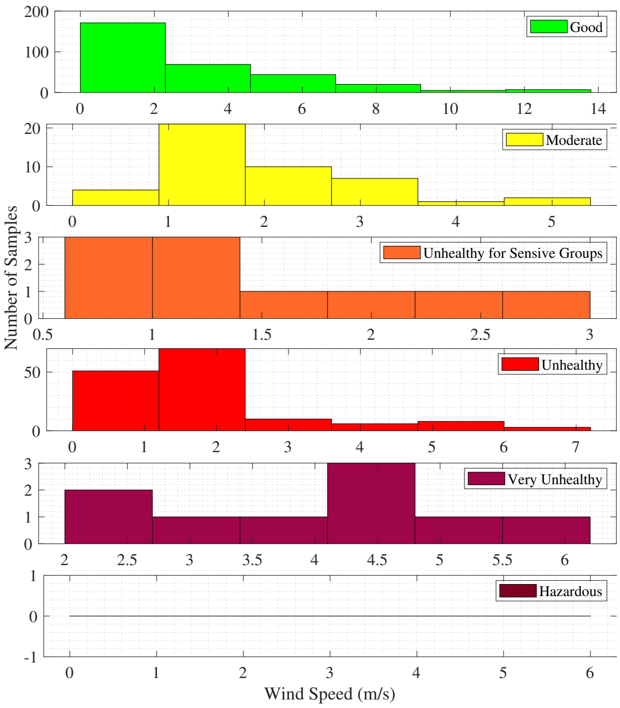

(**c**)

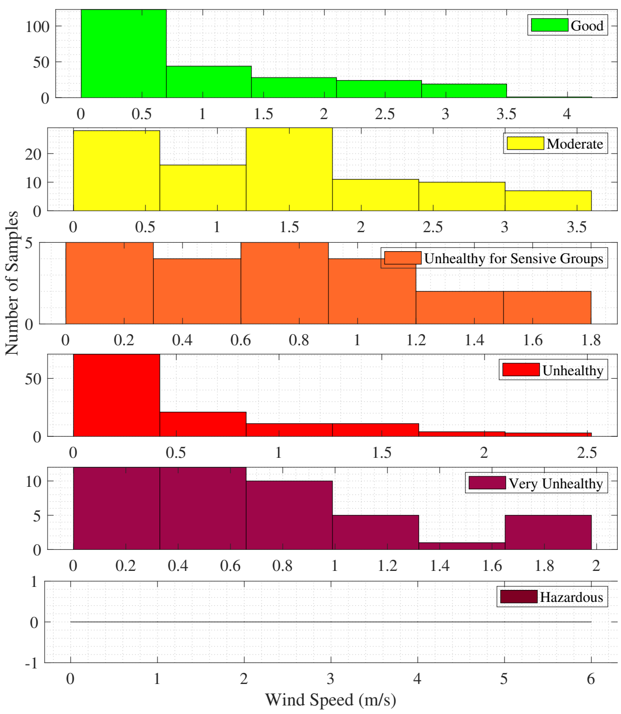

(**d**)

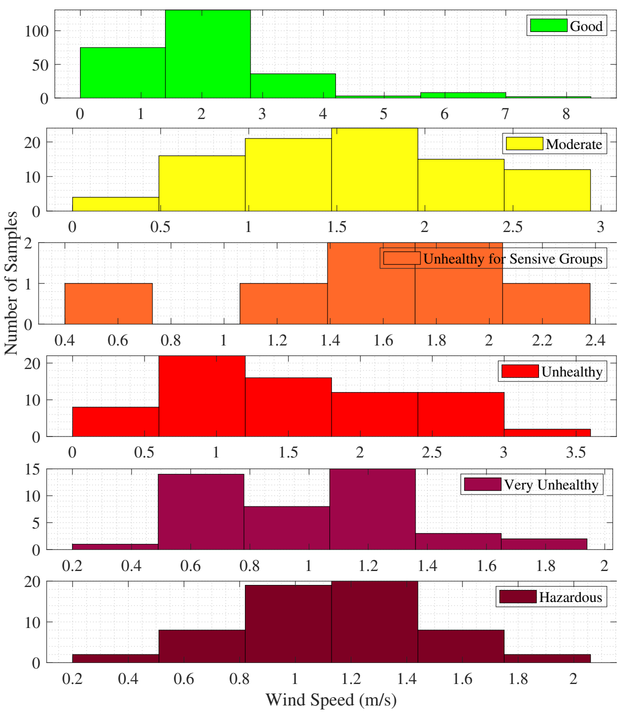

(**e**)

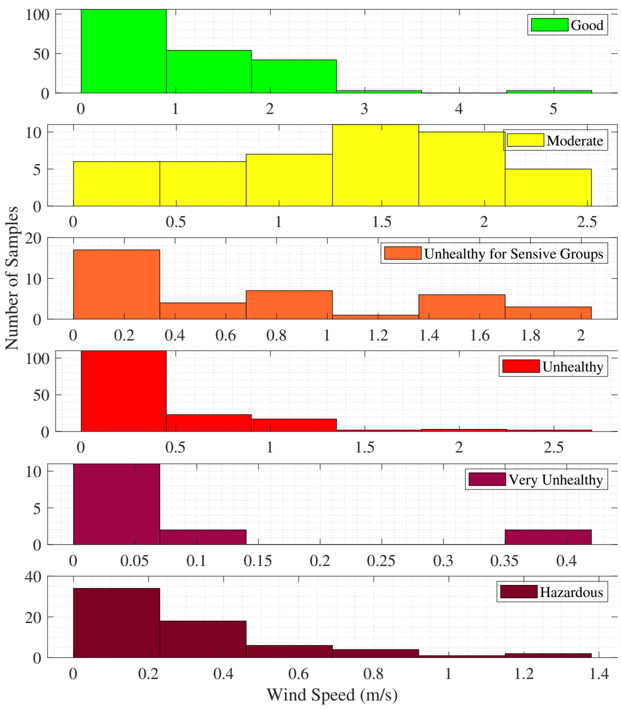

(**f**)

Figure 13. Wind speed histograms for the cities of (**a**) Everett, (**b**) Long Beach, (**c**) Pullman, (**d**) Puyallup, (**e**) Spokane, and (**f**) Wenatchee, divided by the PM 2.5 AQI categories.

The results show that the wind speed values tend to be lower than the average during the periods of high wildfire smoke concentration. As a consequence, wind power generation may be significantly reduced when the air quality is degraded. This, in turn, may lead power system operators to resort to fossil-fuel-fired power generators, which can further worsen the air quality in the affected locations.

5. Conclusions

Wildfires are a concerning risk for human and wildlife safety in terms of the resilient operation of the electric power grid in many regions. Even though solar power generation facilities may not be located in high-fire-risk zones, they may still be affected by the traveling smoke from far away wildfires, affecting large geographic regions. In order to evaluate the impact of the wildfire smoke on solar energy during the 2020 Washington state wildfire season, the AOT and PM2.5 AQI were considered to correlate with the loss of sun irradiance, verifying the impact on solar irradiance and solar power production.

Furthermore, the wind speed average during harsh air quality periods was verified to be at least 17% slower than the periods of good PM 2.5 AQI, reaching a high of more than a 45% decrease, on average, for the city of Wenatchee.

In summary, our work shows that PV production can be significantly impacted during the periods of increased concentration of wildfire smoke and reduced wind speeds, thus highlighting the need for more resilient preparation and planning for wildfire events, especially for policymakers, infrastructure planners, and power system operators who seek to promote and integrate clean and renewable energy sources with increased reliability and resilience.

Further studies can be conducted to analyze different power system operation strategies for locations affected by wildfire smoke considering various power generation options and their impact on air quality levels.

Author Contributions: All authors planned this study and experiments; J.C.d.P. contributed to writing the manuscript and overall supervision of the project; A.Z.B. and T.P. conducted the modeling experiments, performed the analysis, and prepared the text and graphics for the manuscript. All authors have read and agreed to the published version of the manuscript.

Funding: This document is the result of a research project funded by a Washington State University Vancouver Minigrant.

Institutional Review Board Statement: Not applicable.

Informed Consent Statement: Not applicable.

Data Availability Statement: All the data used in this work is freely available online. The Washington State University (WSU) AgWeatherNet (AWN) database contains weather-related data from different weather stations in the state of Washington [35]. The PM 2.5 data was obtained from the Washington State Department of Ecology [36]. The AOT data was collected from the Modern-Era Retrospective analysis for Research and Applications, Version 2 (MERRA-2), available in [37].

Conflicts of Interest: The authors declare no conflict of interest.

Abbreviations

The following abbreviations are used in this manuscript:

AOT	Aerosol optical thickness
AQI	Air quality index
AWN	AgWeatherNet
CAISO	California Independent System Operator
DNR	Department of Natural Resources
EPA U.S.	Environmental Protection Agency
HMS	Hazard mapping system
MAE	Mean absolute error
MSE	Mean squared error
NOAA	National Oceanic and Atmospheric Administration
PM 2.5	Particular matter 2.5
PV	Photovoltaic
U.S.	United States
VIF	Variance inflation factor
WSU	Washington State University

References

1. Witze, A. The Arctic is burning like never before—and that's bad news for climate change. *Nature* **2020**, *585*. [CrossRef]
2. Wheeling, K. Australia's Most Extreme Bushfire Season, Statistically Speaking. *Eos* **2020**, *101*. [CrossRef]
3. Logiuratto, E. Desperate Race Against Fires in World's Biggest Tropical Wetlands. 2020. Available online: https://phys.org/news/2021-01-brazil-wildfires-surge.html (accessed on 21 December 2021).
4. NIFC. National Fire News. 2020. Available online: https://www.nifc.gov/fire-information/nfn (accessed on 21 December 2021).
5. NIFC. National Interagency Fire Center. 2020. Available online: https://www.nifc.gov/fireInfo/fireInfo_statistics.html (accessed on 21 December 2021).
6. Filonchyk, M.; Peterson, M.P.; Sun, D. Deterioration of air quality associated with the 2020 US wildfires. *Sci. Total Environ.* **2022**, *826*, 154103. [CrossRef]
7. Xiang, J.; Huang, C.H.; Shirai, J.; Liu, Y.; Carmona, N.; Zuidema, C.; Austin, E.; Gould, T.; Larson, T.; Seto, E. Field measurements of PM2.5 infiltration factor and portable air cleaner effectiveness during wildfire episodes in US residences. *Sci. Total Environ.* **2021**, *773*, 145642. [CrossRef] [PubMed]
8. PG&E. Pacific Gas and Electric Company (PG&E) Wildfire Safety. 2020. Available online: https://www.pge.com/en_US/safety/emergencypreparedness/natural-disaster/wildfires/wildfire-safety.page?WT.mc_id=Vanity_wildfiresafety (accessed on 21 December 2021).
9. Case, M.J.; Johnson, B.G.; Bartowitz, K.J.; Hudiburg, T.W. Forests of the future: Climate change impacts and implications for carbon storage in the Pacific Northwest, USA. *For. Ecol. Manag.* **2021**, *482*, 118886. [CrossRef]
10. Abatzoglou, J.T.; Kolden, C.A. Climate change in western US deserts: Potential for increased wildfire and invasive annual grasses. *Rangel. Ecol. Manag.* **2011**, *64*, 471–478. [CrossRef]
11. Liu, Y.; Goodrick, S.L.; Stanturf, J.A. Future U.S. wildfire potential trends projected using a dynamically downscaled climate change scenario. *For. Ecol. Manag.* **2013**, *294*, 120–135. [CrossRef]
12. Brando, P.; Macedo, M.; Silvério, D.; Rattis, L.; Paolucci, L.; Alencar, A.; Coe, M.; Amorim, C. Amazon wildfires: Scenes from a foreseeable disaster. *Flora* **2020**, *268*, 151609. [CrossRef]
13. Rocca, M.E.; Miniat, C.F.; Mitchell, R.J. Introduction to the regional assessments: Climate change, wildfire, and forest ecosystem services in the USA. *Sci. J.* **2014**, *327*, 265–268. [CrossRef]
14. Summers, J.K.; Lamper, A.; McMillion, C.; Harwell, L.C. Observed Changes in the Frequency, Intensity, and Spatial Patterns of Nine Natural Hazards in the United States from 2000 to 2019. *Sustainability* **2022**, *14*, 4158. [CrossRef]
15. Gonick, S.A.; Errett, N.A. Integrating Climate Change into Hazard Mitigation Planning: A Survey of State Hazard Mitigation Officers. *Sustainability* **2018**, *10*, 4150. [CrossRef]
16. Post, T.W. The Washington Post (Sept., 2020), "Wildfire Smoke Reaches Europe". 2020. Available online: https://www.washingtonpost.com/weather/2020/09/16/wildfire-smoke-reaches-europe/ (accessed on 21 December 2021).
17. NOAA. Hazard Mapping System Fire and Smoke Product. 2020. Available online: https://www.ospo.noaa.gov/Products/land/hms.html#0 (accessed on 7 January 2022).
18. Google Maps. Continental United States of America 1 cm : 100mi. Google Maps Online. 2020. Available online: https://www.google.com/maps (accessed on 7 January 2022).
19. Kollanus, V.; Tiittanen, P.; Niemi, J.V.; Lanki, T. Effects of long-range transported air pollution from vegetation fires on daily mortality and hospital admissions in the Helsinki metropolitan area, Finland. *Environ. Res.* **2016**, *151*, 351–358. [CrossRef] [PubMed]
20. World, R.E. Renewable Energy World (Oct., 2020) "California Wildfire Smoke Decreases Solar Generation by More than 13% in CAIS". 2020. Available online: https://www.renewableenergyworld.com/solar/california-wildfire-smokedecreases-solar-generation-by-more-than-13-in-caiso/#gref (accessed on 8 February 2022).
21. C2ES. Center for Climate and Energy Solutions: Renewable Energy. 2020. Available online: https://www.c2es.org/content/renewable-energy/ (accessed on 21 February 2022).
22. Keelin, P.; Kubiniec, A.; Bhat, A.; Perez, M.; Dise, J.; Perez, R.; Schlemmer, J. Quantifying the solar impacts of wildfire smoke in western North America. In Proceedings of the 2021 IEEE 48th Photovoltaic Specialists Conference (PVSC), Fort Lauderdale, FL, USA, 20–25 June 2021; pp. 1401–1404. [CrossRef]
23. Gilletly, S.D.; Jackson, N.D.; Staid, A. Quantifying Wildfire-Induced Impacts to Photovoltaic Energy Production in the western United States. In Proceedings of the 2021 IEEE 48th Photovoltaic Specialists Conference (PVSC), Fort Lauderdale, FL, USA, 20–25 June 2021; pp. 1619–1625. [CrossRef]
24. EIA. Smoke from California Wildfires Decreases Solar Generation in CAISO. 2020. Available online: https://www.eia.gov/todayinenergy/detail.php?id=45336 (accessed on 21 January 2022).
25. Donaldson, D.L.; Piper, D.M.; Jayaweera, D. Temporal Solar Photovoltaic Generation Capacity Reduction from Wildfire Smoke. *IEEE Access* **2021**, *9*, 79841–79852. [CrossRef]
26. Department of Natural Resources. Wildfire Season 2020. 2020. Available online: https://www.dnr.wa.gov/publications/rp_fire_annual_report_2020.pdf (accessed on 7 February 2021).
27. GACC. NWCC Summary, GACC Detailed Situation Report—By Protection. 2020. Available online: https://gacc.nifc.gov/nwcc/content/products/intelligence/sitreport.pdf (accessed on 7 February 2021).

28. NREL. PVWatts Version 5 Manual. 2014. Available online: https://www.nrel.gov/docs/fy14osti/62641.pdf (accessed on 22 December 2021).
29. Kim, G.G.; Choi, J.H.; Park, S.Y.; Bhang, B.G.; Nam, W.J.; Cha, H.L.; Park, N.; Ahn, H.K. Prediction Model for PV Performance with Correlation Analysis of Environmental Variables. *IEEE J. Photovolt.* **2019**, *9*, 832–841. [CrossRef]
30. EPA. Revised Air Quality Standards for Particle Pollution And Updates to the Air Quality Index (Aqi). 2012. Available online: https://www.epa.gov/sites/default/files/2016-04/documents/2012_aqi_factsheet.pdf (accessed on 8 February 2022).
31. David, A.T.; Asarian, J.E.; Lake, F.K. Wildfire Smoke Cools Summer River and Stream Water Temperatures. *Water Resour. Res.* **2018**, *54*, 7273–7290. [CrossRef]
32. NOAA. Global Monitoring Laboratory. Available online: https://gml.noaa.gov/grad/surfrad/aod (accessed on 4 April 2022).
33. Moore, D.S.; McCabe, G.P. *Introduction to the Practice of Statistics*; WH Freeman/Times Books/Henry Holt & Co.: New York, NY, USA, 1989.
34. Manwell, J.F.; McGowan, J.G.; Rogers, A.L. *Wind Energy Explained: Theory, Design and Application*; John Wiley & Sons: Hoboken, NJ, USA, 2010.
35. WSU. AgWeatherNet. 2021. Available online: http://weather.wsu.edu/?p=88650&desktop (accessed on 22 December 2021).
36. DESW. Washington's Air Quality Monitoring Network. 2021. Available online: https://enviwa.ecology.wa.gov/Report/Hr24PM25SummaryNew (accessed on 2 December 2021).
37. GMAO. *Global Modeling Assimilation Office, MERRA-2 tavg1_2d_aer _Nx: 2d, 1-Hourly, Time-averaged, Single-Level, Assimilation, Aerosol Diagnostics V5.12.4*; Goddard Earth Sciences Data and Information Services Center (GES DISC): Greenbelt, MD, USA, 2021. Available online: https://giovanni.gsfc.nasa.gov/giovanni/ (accessed on 2 December 2021). [CrossRef]
38. Menard, S. *Applied Logistic Regression Analysis*; Sage Publications, Inc.: Thousand Oaks, CA, USA, 2001.